PHYSICAL REVIEW D **81,** 055009 (2010)

Light colored scalars from grand unification and the forward-backward asymmetry in $t\bar{t}$ production

Ilja Doršner,[1,*] Svjetlana Fajfer,[2,3,†] Jernej F. Kamenik,[3,‡] and Nejc Košnik[3,§]

[1]*Department of Physics, University of Sarajevo, Zmaja do Bosne 33-35, 71000 Sarajevo, Bosnia and Herzegovina*
[2]*Department of Physics, University of Ljubljana, Jadranska 19, 1000 Ljubljana, Slovenia*
[3]*Jožef Stefan Institute, Jamova 39, P. O. Box 3000, 1001 Ljubljana, Slovenia*

(Received 8 January 2010; published 25 March 2010)

The experimental results on the $t\bar{t}$ production cross section at the Tevatron are well described by the QCD contributions within the standard model, while the recently measured forward-backward asymmetry is larger than predicted within this framework. We consider light colored scalars appearing in a particular $SU(5)$ grand unified theory model within the 45-dimensional Higgs representation. A virtue of the model is that it connects the presence of a light colored $SU(2)$ singlet (Δ_6) and a color octet weak doublet (Δ_1) with bounds on the proton lifetime, which constrain the parameter space of both scalars. We find that both the total $t\bar{t}$ production cross section and the forward-backward asymmetry can be accommodated simultaneously within this model. The experimental results prefer a region for the mass of Δ_6 around 400 GeV, while Δ_1 is then constrained to have a mass around the TeV scale as well. We analyze possible experimental signatures and find that Δ_6 associated top production could be probed in the $t\bar{t}$ + jets final states at Tevatron and the LHC.

DOI: 10.1103/PhysRevD.81.055009 PACS numbers: 12.10.Dm, 13.85.Ni, 14.65.Ha

I. INTRODUCTION

The CDF and D0 experiments at the Tevatron have produced many important and useful results in top quark physics. Recently the measurements of the forward-backward asymmetry in $t\bar{t}$ production (FBA) [1,2] have attracted a lot of attention due to the more than 2σ discrepancy of the most precise experimental result [1] compared to the $\mathcal{O}(\alpha_s^3)$ interference effect predicted within the standard model (SM) [3]. At the same time, other CDF and D0 results on top quark properties and processes exhibit a very good agreement with SM predictions [4]. Several scenarios of new physics (NP) have already been considered, trying to explain this discrepancy [5–8].

Among possible NP proposals, the path of gauge unification in the form of grand unified theories (GUTs) is perhaps one of the most appealing. Traditionally, the two main challenges of GUTs have been achieving SM gauge couplings' unification and ensuring stability of the proton beyond present experimental limits. Recently, nonsupersymmetric $SU(5)$ GUT models [9–11] that incorporate 45-dimensional scalar representation have been found to satisfy the first criterion. An important observation was that some of the 45 states can be relatively light and play an interesting role in ensuring sufficient proton stability. With this in mind, we have recently investigated the role of scalar leptoquarks also appearing within such a representation in charm meson decays [12].

In the present study we investigate a colored $SU(2)_L$ singlet with electric charge $4/3$ (Δ_6), which is incorporated in the 45-dimensional representation of $SU(5)$, as a possible explanation of the FBA discrepancy. Direct experimental constraints on the mass and couplings of the new state come from flavor and collider experiments. In addition however, they are constrained indirectly due to gauge couplings' unification and with the proton not decaying too fast. In particular, it turns out that the later two conditions require another relatively light state (Δ_1), which is an octet of color, doublet of $SU(2)_L$, and has hypercharge one half.

The paper is organized in the following sections: In Sec. II we introduce the candidate $\Delta_{1,6}$ states within a GUT model and discuss constraints coming from gauge couplings' unification and proton decay. In Sec. III we discuss the phenomenology of the two Δ's in hadronic $t\bar{t}$ production at the Tevatron, while other related phenomenology and constraints are discussed in Sec. IV. We briefly cover possible search strategies for Δ_6 at the Tevatron and the LHC in Sec. V, before summarizing our results in Sec. VI.

II. Δ_1 AND Δ_6

The scalar fields we discuss—$(\bar{3}, 1, 4/3)$ and $(8, 2, 1/2)$—naturally emerge in a theoretically well-motivated class of grand unified scenarios. Namely, they both reside in a 45-dimensional scalar representation of $SU(5)$. And, this representation should be a part of any simple renormalizable scenario without supersymmetry

*ilja.dorsner@ijs.si
†svjetlana.fajfer@ijs.si
‡jernej.kamenik@ijs.si
§nejc.kosnik@ijs.si

together with a 5-dimensional scalar representation—$5 \equiv (\Psi_D, \Psi_T) = (1, 2, 1/2) \oplus (3, 1, -1/3)$—to generate viable masses of charged fermions [13]. It is entirely possible to bypass this requirement by either judicious introduction of extra vectorlike fermions [14] or the use of higher dimensional operators to correct charged fermion mass relations. However, both approaches have no unique implementation and, in the latter case, the same class of operators could have significant effect on the gauge coupling unification [15,16]. To avoid these ambiguities we opt for the framework where viable charged fermion masses are generated through 5- and 45-dimensional scalar representations at the tree level and neglect influence of all higher dimensional operators. We accordingly discuss scalar fields in question in their most natural setting—a renormalizable $SU(5)$ framework without supersymmetry—in what follows.

The couplings of the multiplets in the 45-dimensional scalar representation of $SU(5)$—$45 \equiv (\Delta_1, \Delta_2, \Delta_3, \Delta_4, \Delta_5, \Delta_6, \Delta_7) = (8, 2, 1/2) \oplus (\bar{6}, 1, -1/3) \oplus (3, 3, -1/3) \oplus (\bar{3}, 2, -7/6) \oplus (3, 1, -1/3) \oplus (\bar{3}, 1, 4/3) \oplus (1, 2, 1/2)$—to the matter are set by the following pair of $SU(5)$ contractions: $(Y_1)_{ij}(10^{\alpha\beta})_i(\bar{5}_\delta)_j 45^{*\delta}_{\alpha\beta}$ and $\epsilon_{\alpha\beta\gamma\delta\epsilon}(Y_2)_{ij}(10^{\alpha\beta})_i \times (10^{\zeta\gamma})_j(45)^{\delta\epsilon}_{\zeta}$. Y_1 and Y_2 are Yukawa coupling matrices while the matter fields of the SM reside in 10_i and $\bar{5}_j$ [17], where $i, j = 1, 2, 3$ are family indices. The couplings of $(\bar{3}, 1, 4/3) = \Delta_6$ are then

$$\mathcal{L} \ni (Y_1)_{ij} e_i^{CT} C d_{aj}^C \Delta_{6a}^* + \sqrt{2}[(Y_2)_{ij} - (Y_2)_{ji}] \times \epsilon_{abc} u_{ia}^{CT} C u_{bj}^C \Delta_{6c}, \quad (1)$$

where $a, b = 1, 2, 3$ are color indices. Note that the latter set of couplings is antisymmetric in flavor space. It is that fact that makes Δ_6 leptoquarks innocuous as far as the proton decay is concerned at the tree level as has been noticed only recently [12]. Nevertheless, Δ_6 could still mix via the Higgs doublet with a scalar that has the right diquark couplings to destabilize the proton [18]. Indeed, there is one such scalar multiplet in the adjoint representation of $SU(5)$. However, in simple scenarios we have in mind, where there is only one adjoint scalar—$24 \equiv (\Sigma_8, \Sigma_3, \Sigma_{(3,2)}, \Sigma_{(\bar{3},2)}, \Sigma_{24}) = (8, 1, 0) \oplus (1, 3, 0) \oplus (3, 2, -5/6) \oplus (\bar{3}, 2, 5/6) \oplus (1, 1, 0)$—that breaks $SU(5)$, these particular components, i.e., $\Sigma_{(3,2)}$ and $\Sigma_{(\bar{3},2)}$, always get eaten by the so-called X and Y gauge bosons and are thus prohibited from mixing.

The couplings of $(8, 2, 1/2) = \Delta_1$ to the matter are

$$\mathcal{L} \ni -\sqrt{2}(Y_1)_{ij} d_{ai}^T (T^A)_{ab} C d_{bj}^C \Delta_1^{0A*}, -2[(Y_2)_{ij} - (Y_2)_{ji}] \times u_{ai}^T (T^A)_{ab} C u_{bj}^C \Delta_1^{0A}, -\sqrt{2}(Y_1)_{ij} u_{ai}^T (T^A)_{ab} C d_{bj}^C \Delta_1^{+A*} + 2[(Y_2)_{ij} - (Y_2)_{ji}] d_{ai}^T (T^A)_{ab} C u_{bj}^C \Delta_1^{+A}. \quad (2)$$

Here, $(T^A)_{ab} = 1/2(\lambda^A)_{ab}$, where λ^A $(A = 1, \ldots, 8)$ are the usual Gell-Mann matrices of $SU(3)$. Δ_1 has two sets of color components. One is electrically neutral—Δ_1^{0A}—and the other is electrically charged—Δ_1^{+A}.

Clearly, both Δ_1 and Δ_6 have the right couplings to influence the asymmetry we are interested in. However, in order to be relevant both Δ_1 and Δ_6 must be sufficiently light. This, on the other hand, has repercussions for unification of gauge couplings. In particular, Δ_6 tends to either lower the unification scale below proton decay limits or ruin gauge coupling unification all together if light enough. On the other hand, the Δ_1 mass scale and the GUT scale, i.e., scale where the SM couplings unify, are inversely proportional. So, whenever Δ_6 is light Δ_1 will also be light in order to keep the GUT scale above the limits imposed by proton decay. In other words, whenever Δ_6 is light enough to play a role in low energy physics the same is true for Δ_1.

We find that the simplest $SU(5)$ scenario comprising only 5-, 24-, and 45-dimensional scalar representations cannot unify at all with Δ_6 light. (Admittedly, the scenario with this content when Δ_6 is sufficiently heavy unifies [9,10,19] but is already ruled out by proton decay experiments according to a recent study [9] unless one suppresses relevant operators due to either scalar [12] or gauge boson exchange [20] or both.) Of course, one can always judiciously add an arbitrary number of additional representations of various dimensions to adjust for that but we seek a theoretically well-motivated scenario. We have accordingly checked unification with light Δ_6 in the following two simple $SU(5)$ scenarios where all the standard model fermions have viable masses and mixing parameters.

First, we have studied a scenario where, in addition to the 5-, 24-, and 45-dimensional scalar representations, we have a 15-dimensional scalar representation [9,10] to generate neutrino masses via the type II seesaw mechanism [21–24]. In this case, the gauge couplings of the SM do unify but the GUT scale comes out too low. Namely, the upper bound turns out to be around 10^{13} GeV which implies that the masses of X and Y gauge bosons—mediators of proton decay—are unacceptably small.

We have then replaced the 15-dimensional scalar representation with a 24-dimensional fermionic representation—$24_F \equiv (\rho_8, \rho_3, \rho_{(3,2)}, \rho_{(\bar{3},2)}, \rho_{24}) = (8, 1, 0) \oplus (1, 3, 0) \oplus (3, 2, -5/6) \oplus (\bar{3}, 2, 5/6) \oplus (1, 1, 0)$—to have a renormalizable $SU(5)$ scenario [11] where neutrino masses are generated via combination of type I [25–29] and type III [30,31] seesaw mechanisms. (This is a renormalizable version of the model proposed in [32] and further analyzed in [33].) In that particular scenario, the situation is much more promising. Namely, the upper bound on the GUT scale comes out very close to the present experimental limits due to partial proton decay lifetime measurements with both Δ_1 and Δ_6 in the range accessible in collider experiments. Since the unification in this regime is very constraining and rich in features we discuss it in some details next.

For the unification of the SM gauge couplings at the GUT scale ($M_{\rm GUT}$) to be successful at the one loop level two relevant equations [19] need to be satisfied:

$$\frac{B_{23}}{B_{12}} = \frac{5}{8}\frac{\sin^2\theta_W - \alpha/\alpha_3}{3/8 - \sin^2\theta_W} = 0.716 \pm 0.005, \quad (3a)$$

$$B_{12} = \frac{16\pi}{5\alpha}(3/8 - \sin^2\theta_W) = 184.9 \pm 0.2. \quad (3b)$$

The right-hand sides reflect the latest experimental measurements of the SM parameters [34] at M_Z in the $\overline{MS}$ scheme: $\alpha_3 = 0.1176 \pm 0.0020$, $\alpha^{-1} = 127.906 \pm 0.019$, and $\sin^2\theta_W = 0.231\,22 \pm 0.000\,15$. The left-hand sides, on the other hand, depend on particle content and associated mass spectrum of the particular unification scenario. In fact, $B_{ij} = B_i - B_j$, where $B_i = \sum_I b_{iI} \ln M_{\rm GUT}/m_I$, ($M_Z \leq m_I \leq M_{\rm GUT}$). The sum over I goes over all particles from M_Z—the SM particle scale—to the GUT scale. b_{iI} are the usual β-function coefficients of the particle I of mass m_I. For example, the SM content with one light Higgs doublet field has $b_1 = 41/10$, $b_2 = -19/6$, and $b_3 = -7$, and, accordingly, yields $B_{23}/B_{12} \approx 0.53$.

Any potentially realistic $SU(5)$ grand unified scenario must also allow for large enough masses of the X and Y gauge bosons since these vector leptoquarks mediate proton decay. Their practically degenerate masses are identified with $M_{\rm GUT}$ ($m_{(X,Y)} \equiv M_{\rm GUT}$), which in turn allows one to set lower bound on the GUT scale using proton decay lifetime limits. The most stringent bound comes from the latest experimental limit [35] on $p \to \pi^0 e^+$ partial decay lifetime: $\tau_{p\to\pi^0 e^+} > 8.2 \times 10^{33}$ years. Theoretical prediction for this particular channel reads

$$\Gamma \approx \frac{m_p}{f_\pi^2}\frac{\pi}{4}A_L^2|\alpha|^2(1 + D + F)^2\frac{\alpha_{\rm GUT}^2}{m_{(X,Y)}^4}[A_{SR}^2 + 4A_{SL}^2], \quad (4)$$

where $A_{SL(R)}$ gives a leading-log renormalization of the relevant operators from the GUT scale to M_Z. These are given as [36–38]

$$A_{SL(R)} = \prod_{i=1,2,3}\prod_{I}^{M_Z\leq m_I\leq M_{\rm GUT}}\left[\frac{\alpha_i(m_{I+1})}{\alpha_i(m_I)}\right]^{(\gamma_{L(R)i})/(\sum_J^{M_Z\leq m_J\leq m_I} b_{iJ})}, \quad (5)$$

where $\gamma_{L(R)i} = (23(11)/20, 9/4, 2)$. The QCD running below M_Z is captured by the coefficient A_L. To establish lower bound on $M_{\rm GUT}$ we further use $m_p = 938.3$ MeV, $D = 0.81$, $F = 0.44$, $f_\pi = 139$ MeV, $A_L = 1.25$, and $|\alpha| = 0.01$ GeV^3 [39].

Also, the masses of all scalar leptoquarks that mediate proton decay must be sufficiently heavy to render the scenario viable. These are Ψ_T, Δ_3, and Δ_5. (Note that Δ_6 has erroneously been associated with a generation of the so-called $d = 6$ proton decay operators [18].) If all the couplings of 45 with matter are taken into account [12] and no suppression via Yukawa couplings is arranged their masses should not be below 10^{12} GeV due to the proton decay constraints. To remind us of that we place a line over them in Table I for convenience where we list all nontrivial $b_i - b_j$ contributions of the scenario we analyze.

In addition to these considerations there are two more constraints on the mass spectrum of the particles listed in Table I. First, ρ_8 must be heavier than 10^6 GeV to accommodate the big bang nucleosynthesis constraints [32]. Second, in the renormalizable model we are interested in [11] there is a particular relation between masses of the fields in fermionic adjoint. Namely, due to a small number of terms in the relevant part of the Lagrange density the masses of these fields are not independent from each other [11]. As it turns out, we get unification only in one regime when Δ_6 is light which corresponds to the following set of mass relations [11]:

$$m_{\rho_8} = \hat{m} m_{\rho_3}, \qquad m_{\rho_{(3,2)}} = m_{\rho_{(\bar{3},2)}} = \frac{(1+\hat{m})}{2}m_{\rho_3}, \quad (6)$$

where $\hat{m}$ is a free parameter that basically represents a measure of the mass splitting between ρ_8 and ρ_3.

With all these constraints in mind we are now in a position to determine an upper bound on the GUT scale at the one loop level assuming that Δ_6 is responsible for asymmetry and is accordingly in the following mass range: 300 GeV $\leq m_{\Delta_6} \leq 1$ TeV (see Sec. III for details). We do that by numerically maximizing $M_{\rm GUT}$ while imposing that solution that not only satisfies Eqs. (3a), (3b), and (6) but that the masses given by numerical solution are in the following ranges: 10^2 GeV $\leq m_{\Sigma_3}, m_{\Sigma_8}, m_{\Delta_1}, m_{\Delta_2}, m_{\Delta_4}, m_{\Delta_7}, m_{\rho_{(3,2)}}, m_{\rho_{(\bar{3},2)}} \leq M_{\rm GUT}$, 10^{12} GeV $\leq m_{\Psi_T}, m_{\Delta_3}, m_{\Delta_5} \leq M_{\rm GUT}$ and 10^6 GeV $\leq m_{\rho_8} \leq M_{\rm GUT}$.

In Fig. 1 (Fig. 2) we present the $\hat{m} = 10^{14}$ ($\hat{m} = 10^{12}$) scenario. We opt for this because in the region of parameter space we are interested in, i.e., 300 GeV $\leq m_{\Delta_6} \leq 1$ TeV, viable unification can exist only when $10^{6.4} \leq \hat{m} \leq 10^{14.2}$. However, if $M_{\rm GUT}$ is to be above the limit imposed by proton decay measurements then $10^{11.5} \leq \hat{m} \leq 10^{14.2}$.

TABLE I. The $b_i - b_j$ coefficient contributions.

	Ψ_D	$\bar{\Psi}_T$	Σ_8	Σ_3	Δ_1	Δ_2	$\bar{\Delta}_3$	Δ_4	$\bar{\Delta}_5$	Δ_6	Δ_7	ρ_8	ρ_3	$\rho_{(3,2)} + \rho_{(\bar{3},2)}$
b_{23}	$\frac{1}{6}$	$-\frac{1}{6}$	$-\frac{3}{6}$	$\frac{2}{6}$	$-\frac{4}{6}$	$-\frac{5}{6}$	$\frac{9}{6}$	$\frac{1}{6}$	$-\frac{1}{6}$	$-\frac{1}{6}$	$\frac{1}{6}$	$-\frac{12}{6}$	$\frac{8}{6}$	$\frac{4}{6}$
b_{12}	$-\frac{1}{15}$	$\frac{1}{15}$	0	$-\frac{5}{15}$	$-\frac{8}{15}$	$\frac{2}{15}$	$-\frac{27}{15}$	$\frac{17}{15}$	$\frac{1}{15}$	$\frac{16}{15}$	$-\frac{1}{15}$	0	$-\frac{20}{15}$	$\frac{20}{15}$

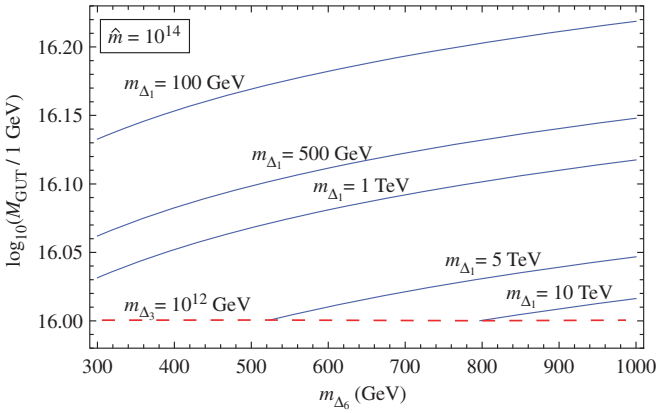

FIG. 1 (color online). Viable unification in the $\hat{m} = 10^{14}$ case. The allowed region is between $m_{\Delta_1} = 10^2$ GeV and the dashed line, which is due to the constraint imposed by experimental results on proton decay when imposed on the p decay predictions due to the scalar boson exchange.

It is important to stress that for each viable unification point in Figs. 1 and 2 we know the full mass spectrum of the model including $\alpha_{\rm GUT}$ and $A_{SL(R)}$. We can thus establish an accurate lower bound on $M_{\rm GUT}$ by matching the prediction of the scenario for a partial lifetime of $p \to \pi^0 e^+$ at the leading order due to the gauge boson exchange with the current experimental limit. This prediction is seen in Fig. 2 as a dashed line. Space below that line should be considered as excluded. In Fig. 1, however, an almost horizontal dashed line represents a line along which the mass of proton decay mediating scalar Δ_3 is at its experimentally imposed limit ($m_{\Delta_3} = 10^{12}$ GeV). Again, space below that line should be considered as excluded. What happens is that as $\hat{m}$ is varied we go from one regime where the so-called $d = 6$ proton decay operators due to gauge boson exchange dominate ($\hat{m} = 10^{14}$) to the other regime where the $d = 6$ proton decay operators due to scalar exchange dominate. The important consequence of this flip in proton decay dominance is that the entire viable region of unification when 300 GeV $\leq m_{\Delta_6} \leq 1$ TeV will be experimentally excluded with an improvement of about a factor of 6 in partial lifetime measurement for $p \to \pi^0 e^+$. This is what makes regime of light Δ_6 extraordinarily predictive and testable.

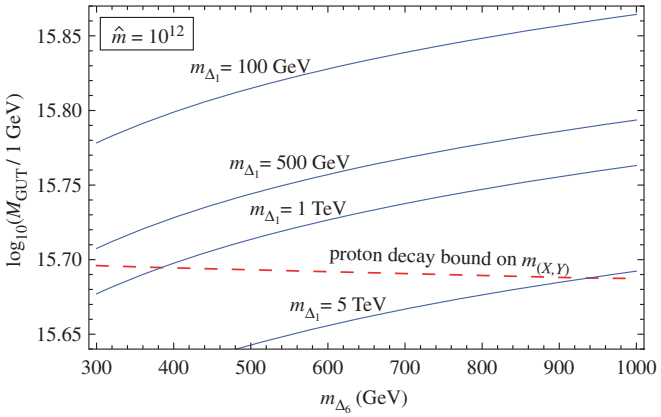

FIG. 2 (color online). Viable unification in the $\hat{m} = 10^{12}$ case. The phenomenologically allowed region is between $m_{\Delta_1} = 10^2$ GeV and the dashed line, which stands for the lower bound on $M_{\rm GUT}$ due to the $d = 6$ proton decay via gauge boson exchange.

Clearly, for a given value of m_{Δ_6} (and $\hat{m}$) we have an upper bound on m_{Δ_1}. For example, when $m_{\Delta_6} = 520$ GeV and $\hat{m} = 10^{14}$ (Fig. 1) we have $m_{\Delta_1} \leq 5$ TeV.

Our findings on unification in the setup with 5-, 24-, and 45-dimensional scalar representations and one adjoint fermionic representation substantially differ from what has been presented elsewhere [40]. In particular, if Δ_6 is not assumed to be light we find no reasonably accessible upper bound on $M_{\rm GUT}$ nor any upper bound on m_{Δ_1}, contrary to what has been put forth in Ref. [40]. To illustrate our disagreement with respect to the $M_{\rm GUT}$ predictions we plot in Fig. 3 what we find to be upper bound on the GUT scale as a function of $\hat{m}$ for varying values of m_{Δ_6}. For definiteness we want to compare our finding with those of Ref. [40] when the masses in the fermionic adjoint obey Eq. (6) and $m_{\Delta_1} = 200$ GeV, $m_{\Delta_3} = 10^{12}$ GeV, and $m_{\Delta_6} = M_{\rm GUT}$. Clearly, in the upper bound on $M_{\rm GUT}$ we find when $m_{\Delta_6} = M_{\rm GUT}$ depends strongly on $\hat{m}$ and substantially exceeds the value of 7.8×10^{15} GeV that has been advertised in Ref. [40] as an absolute upper bound in that case. Moreover, the corresponding experimental bound due to proton decay on $M_{\rm GUT}$ (dotted line) for the $m_{\Delta_6} = M_{\rm GUT}$ case is more than 2 orders of magnitude below the predicted value for $M_{\rm GUT}$ in a substantial part of available parameter space. Only when $\hat{m} < 1$ do we actually get a scenario that can be probed by proton decay.

If, however, we assume that m_{Δ_6} is light—as we do—the picture changes completely. The red solid line represents the upper bound on $M_{\rm GUT}$ for $m_{\Delta_6} = 300$ GeV while the

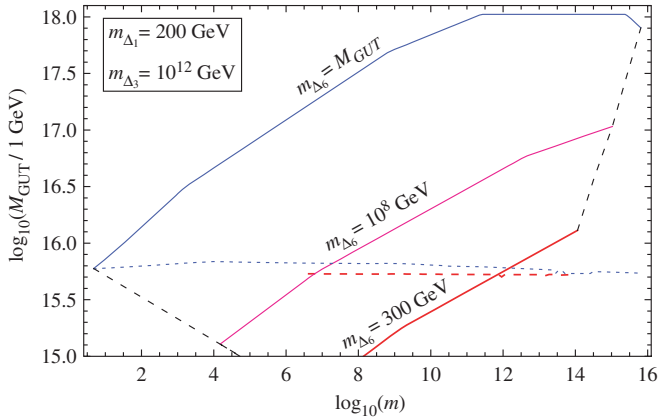

FIG. 3 (color online). Upper bound on $M_{\rm GUT}$ as a function of $\hat{m}$ for different values of m_{Δ_6}.

dashed line represents the corresponding proton decay limit on the GUT scale. Clearly, significant parts of parameter space in this regime are already excluded by proton decay experiments. (Note also that the unification is not possible for all values of $\hat{m}$. Both upper and lower bounds on $\hat{m}$ as a function of m_{Δ_6} are given as thin dashed lines.)

We trace the above mentioned disagreement to a simple fact that the analysis in Ref. [40] does not vary all the masses of the fields in the model within their phenomenologically allowed ranges but makes the judicious choice of varying only those masses that are associated with fields with negative b_{12} coefficients and members of the adjoint fermionic representation. What we have presented is a consistent unification analysis at the one loop level. If one is to consider two loop effects in the running of gauge couplings the relevant range of allowed masses for m_{Δ_6} and m_{Δ_1} would slightly change but they would still be within the TeV range.

III. THE $t\bar{t}$ PRODUCTION CROSS SECTION AND THE FORWARD-BACKWARD ASYMMETRY

In this section we investigate the impact of light $\Delta_{1,6}$ states on the production of $t\bar{t}$ pairs at the Tevatron. The analysis is performed in a model independent way and the results apply to any model scenarios with light colored scalar triplets and/or octets. The current versions of widely used Monte Carlo tools for colliders such as MADGRAPH/MADEVENT and CALCHEP cannot handle the color flow of the required Δ_6 couplings [41]. Therefore we consider LO inclusive production cross sections on which we do not impose any kinematical cuts. A more realistic evaluation would also need to properly simulate particle decays, hadronic showering of their products, and detector effects, all of which can in principle affect the quantities under study. However, we have checked that our calculation of the $t\bar{t}$ production in the SM agrees well with results from MADEVENT. This gives us confidence in the reliability of our crude approach.

The Δ_6 contributes to the $t\bar{t}$ production from the u-channel exchange in the left diagram on Fig. 4. It interferes with the SM $q\bar{q}$ contribution for the $u\bar{u}$ and $c\bar{c}$ initial partons yielding

$$\frac{d\sigma_6^{q\bar{q}}(\hat{s})}{d\hat{t}} = \frac{d\sigma_{\rm SM}^{q\bar{q}}(\hat{s})}{d\hat{t}} - \frac{\alpha_s |g_6^{qt}|^2}{9\hat{s}^3} \frac{(m_t^2\hat{s} + (m_t^2 - \hat{u})^2)}{(m_{\Delta_6}^2 - \hat{u})} + \frac{|g_6^{qt}|^4}{48\pi s^2} \frac{(m_t^2 - \hat{u})^2}{(m_{\Delta_6}^2 - \hat{u})^2}, \tag{7}$$

where $\hat{t} = (p_u - p_t)^2$, $\hat{u} = (p_{\bar{u}} - p_t)^2$ and we have denoted the relevant parameters of the Δ_6 as $g_6^{qt} \equiv 2\sqrt{2}(Y_2^{qt} - Y_2^{tq})$ for $q = u, c$. Similarly the Δ_1 contribution can be obtained by reversing the color and fermion flow of t quarks as seen in the right diagram of Fig. 4 and adjusting

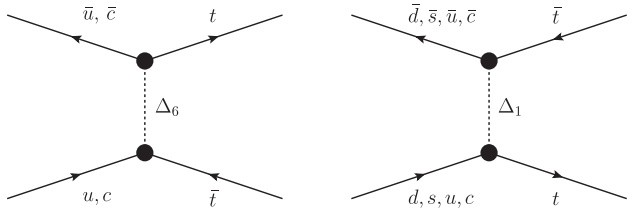

FIG. 4. Leading contributions to the $t\bar{t}$ production cross section and the FBA at the Tevatron coming from Δ_6 (left panel) and Δ_1 (right panel) exchange.

the required color factors. The differential cross section can then be written as

$$\frac{d\sigma_1^{q\bar{q}}(\hat{s})}{d\hat{t}} = \frac{d\sigma_{\rm SM}^{q\bar{q}}(\hat{s})}{d\hat{t}} + \frac{2\alpha_s |g_1^{qt}|^2}{27\hat{s}^3} \frac{(m_t^2\hat{s} + (m_t^2 - \hat{t})^2)}{(m_{\Delta_1}^2 - \hat{t})} + \frac{|g_1^{qt}|^4}{18\pi s^2} \frac{(m_t^2 - \hat{t})^2}{(m_{\Delta_1}^2 - \hat{t})^2}, \tag{8}$$

where now also the down quark partons contribute to the Δ_1 mediated cross section terms. We denote $g_1^{ut} \equiv 4(Y_2^{ut} - Y_2^{tu})$ and $g_1^{dt} \equiv 4\sqrt{(Y_2^{dt} - Y_2^{td})^2 + Y_1^{dt*2}/8}$, where u actually stands for u, c quark flavors and d for d, s. In our analysis we neglect possible interference contributions between both Δ's.

In order to obtain the hadronic cross section, we convolute the partonic result with the appropriate parton distribution functions (PDFs) and consistently transform the phase-space integration from the parton to the lab frame. We obtain

$$\frac{d\sigma(s)}{dt} = \sum_{p,p'=q,g} \int_{x_0}^1 dx_1 \int_{x_0}^1 dx_2 x_1 x_2 \frac{d\sigma^{pp'}(\hat{s})}{d\hat{t}} \times f_p(x_1) f_{p'}(x_2), \tag{9}$$

where $f_p(x)$ is the (anti)proton PDF for parton p, $x_0 = 4m_t^2/s$ is the physical PDF threshold cutoff for our process, $\hat{s} = x_1 x_2 s$ and $\hat{t} = x_1 x_2 (t - m_t^2) + m_t^2$ is the transformed Mandelstam variable $\hat{t} = (p_t - p_{p'})^2$. The factor $x_1 x_2$ in the integrand is the corresponding Jacobian. In the x_1, x_2 integration we have to furthermore impose kinematical limits $\hat{s} > 4m_t^2$ and $-\hat{s}(1 + \hat{\beta}_t)/2 + m_t^2 < \hat{t} < -\hat{s}(1 - \hat{\beta}_t)/2 + m_t^2$, where $\hat{\beta}_t = \sqrt{1 - 4m_t^2/\hat{s}}$. The sum runs over all q quarks as well as antiquark flavors and the gluon contribution, however as discussed above, relevant leading contributions only involve diagonal $p = \bar{p}' = q$ and (in the SM) $p = p' = g$ entries. Finally, to obtain the polar angle (θ) distribution of $t\bar{t}$ pairs, we transform the above differential cross section to

$$\frac{d\sigma(s)}{d\cos\theta} = \frac{s\beta_t}{2} \frac{d\sigma(s)}{dt(\cos\theta)}, \tag{10}$$

where $t(\cos\theta) = -s(1 - \cos\theta\beta_t)/2 + m_t^2$. The FBA and

the total inclusive cross section are then defined as

$$A_{FB}^{t\bar{t}}(s) = \frac{\int_0^1 d\cos\theta[\frac{d\sigma(s)}{d\cos\theta}] - \int_{-1}^0 d\cos\theta[\frac{d\sigma(s)}{d\cos\theta}]}{\sigma_{t\bar{t}}(s)}, \quad (11)$$

$$\sigma_{t\bar{t}}(s) = \int_{-1}^{1} d\cos\theta\left[\frac{d\sigma(s)}{d\cos\theta}\right]. \quad (12)$$

Applying these formulas at the partonic level, it becomes clear that the couplings of the octet Δ_1 cannot induce a large positive FBA. This is also seen on Fig. 5, where we plot examples of the partonic cross section and the FBA induced by the two Δ's, for two different $\Delta_{1,6}$ masses. The Δ_1 contributions interfere constructively with the SM amplitude resulting in big enhancements in the cross section, while the induced FBA is negative. On the other hand, Δ_6 tends to produce a large positive asymmetry at large values of partonic center of mass energy, while the induced asymmetry is negative close to the threshold. Therefore, in order to obtain a good fit to both the cross section and the FBA the contributions of Δ_1 should generically be suppressed compared to those of Δ_6. This would be the case if Δ_1 was much heavier than Δ_6. However, this possibility is limited in this model, by the existing proton decay bounds. Consequently, some fine-tuning is needed between the couplings of Δ_1 to up and down quarks in order to suppress its effects.

In our numerical analysis we use the CTEQ5 [42] set of PDF's at the single renormalization and factorization scale $\mu_F = \mu_R = m_t$ at which we also evaluate the strong coupling constant $\alpha_s(m_t) = 0.108$. We use $m_t = 175$ GeV—the value used by the CDF analysis [43], and rescale our results so that our (tree level) SM value agrees with the SM prediction at next-to-leading order in QCD for $\sigma_{t\bar{t}}(s)$ [44]. We apply the same procedure for each bin when looking at the invariant $t\bar{t}$ mass ($m_{t\bar{t}}$) spectrum and take the reference SM predictions from [45].

We plot the cross section and the FBA at the Tevatron in Fig. 6 as a function of the g_6^{ut} coupling for three Δ_6 masses. We compare the FBA to the difference between the measured value and the SM prediction $A_{FB}^{\rm exp} - A_{FB}^{\rm SM} = (14.2 \pm 6.9)\%$, while we use the CDF cross section value of $\sigma_{t\bar{t}}^{\rm exp} = 7.0 \pm 0.6$ pb [43]. We see that the values for the g_6^{ut} coupling, required to explain the measured FBA are quite large and are positively correlated with m_{Δ_6} so that the

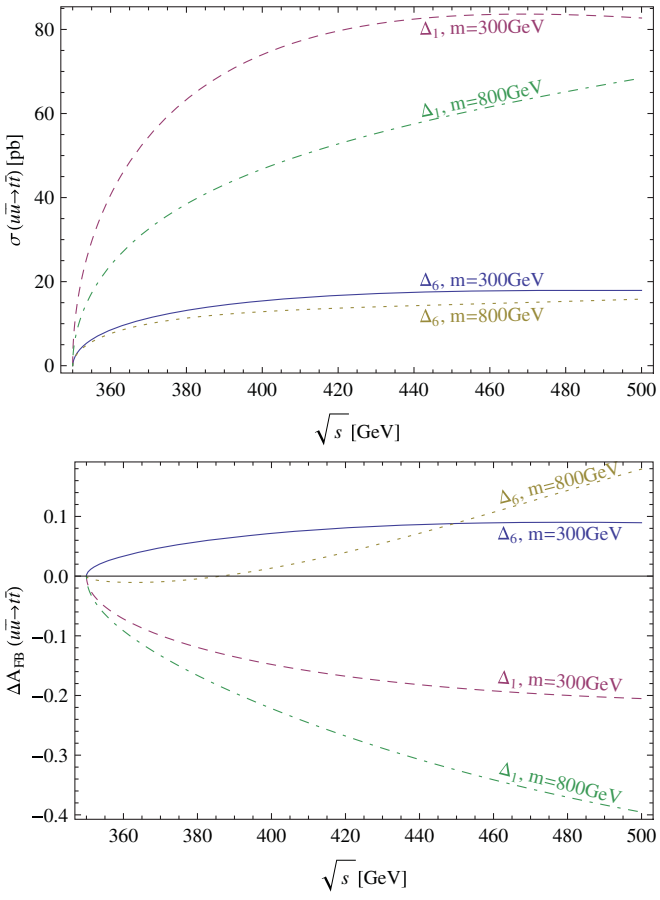

FIG. 5 (color online). Examples of the partonic $t\bar{t}$ cross section (top panel) and the contribution to the FBA (bottom panel), induced by the exchange of $\Delta_{1,6}$.

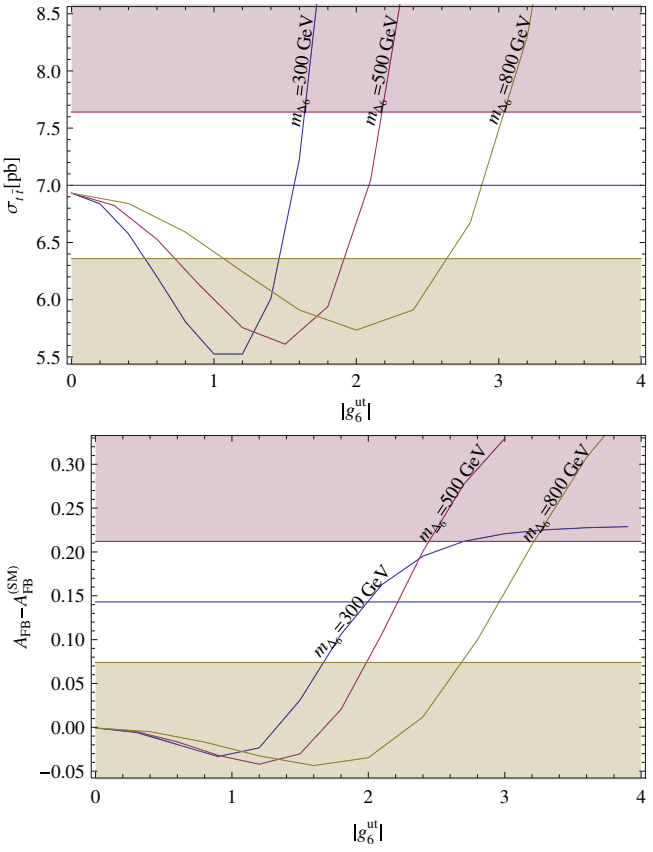

FIG. 6 (color online). Examples of the hadronic $t\bar{t}$ cross section and the FBA at the Tevatron including Δ_6 contributions. The shaded regions are outside the one sigma experimental bounds. For the FBA, the SM contribution is subtracted from the plotted values.

mass of Δ_6 should be right at the electroweak scale to avoid g_6^{ut} becoming nonperturbative. While Δ_6 also contributes in the $c\bar{u}$ and $u\bar{c}$ channels, there is no interference with the leading SM contribution, so that only the last term in Eq. (7) would remain with the coupling replacement $|g_6^{qt}|^4 \to |g_6^{ct} g_6^{ut*}|^2$. Because of the small c and $\bar{c}$ PDF components these contributions are further suppressed. For the same reason the $c\bar{c}$ component contribution cannot significantly affect the cross section for reasonable values of Δ_6 parameters and we are left with the $u\bar{u}$ contribution. The combined constraints on the parameter space of the model given by the integrated $t\bar{t}$ production cross section and the total FBA are shown in Fig. 7. We obtain that both the $t\bar{t}$ production cross section and the FBA can be accommodated simultaneously due to the negative interference contribution to the cross section, provided $m_{\Delta_6} \geq 300$ GeV. The corresponding best-fit relation between the parameters g_6^{ut} and m_{Δ_6} in this region can be put into the approximate form

$$|g_6^{ut}| = 0.9(2) + 2.5(4)\frac{m_{\Delta_6}}{1\ \text{TeV}}. \tag{13}$$

Another important constraint on the relevant parameters of Δ_6 in $t\bar{t}$ production, in particular, its mass, comes from the high $m_{t\bar{t}}$ spectrum measured by the CDF collaboration [46] which reports $\sigma^{t\bar{t}}(800\ \text{GeV} \leq m_{t\bar{t}} \leq 1400\ \text{GeV}) = 0.041 \pm 0.021$ pb, where we have given the integrated cross section in the highest bin and combined the experimental errors of [46] in quadrature. This constraint is shown in Fig. 8 together with the contours of the FBA fit. We see that there is some tension between this constraint and the FBA fit throughout the relevant mass range. The most interesting region lies around $m_{\Delta_6} \approx 400$ GeV where the tension is the smallest. It grows stronger for larger Δ_6 masses and the two observables cannot both be reconciled for m_{Δ_6} above the TeV scale. However, due to the questionable reliability of our naively corrected LO estimation

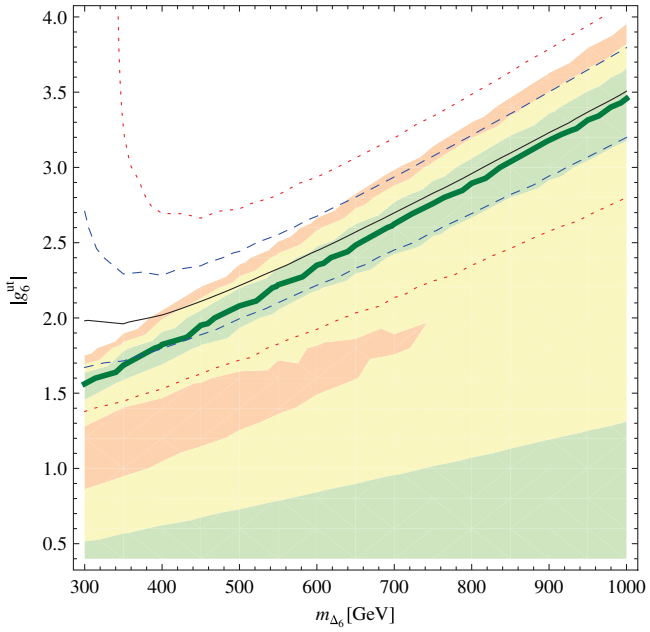

FIG. 7 (color online). Combined constraints on the parameter space of Δ_6 given by the integrated $t\bar{t}$ production cross section (shaded regions) and the total FBA (contours). The 68%, 95%, 99% confidence level regions in production cross section are shaded in green, yellow, and orange, respectively. The corresponding 68(95)% C.L. regions in the FBA are bounded by blue dashed (red dotted) contours. The best-fit contours are drawn in thick (thin) full lines for the cross section and the FBA, respectively.

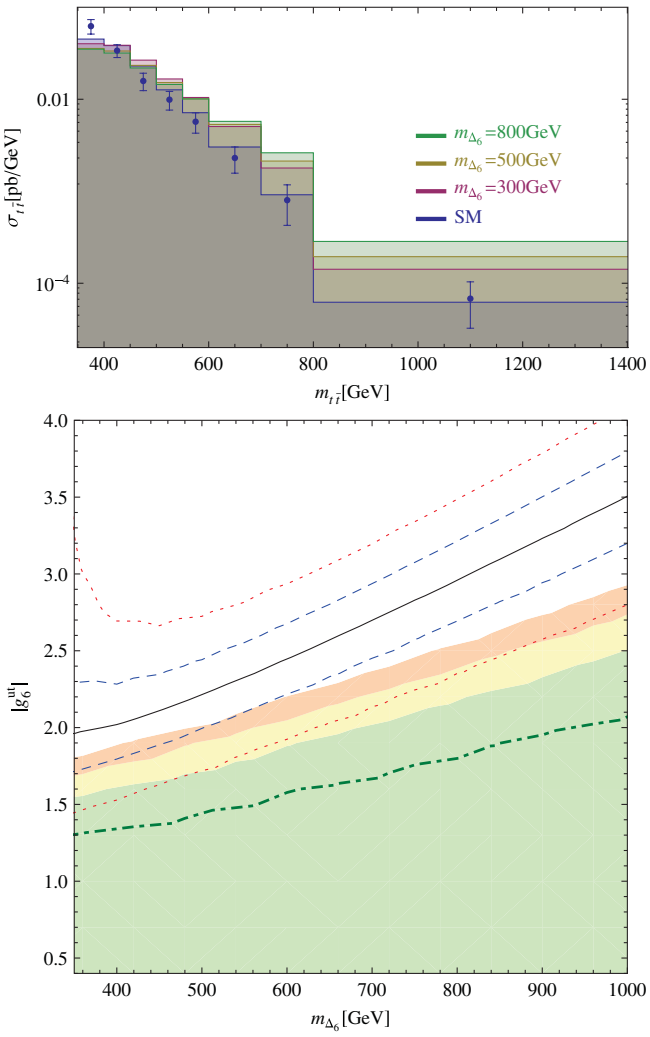

FIG. 8 (color online). Δ_6 contributions to the $m_{t\bar{t}}$ invariant mass spectrum in $t\bar{t}$ production at the Tevatron (top panel) and the resulting constraints on the parameter space (bottom panel). In the top plot, values of g_6^{ut} are chosen according to Eq. (13). In the bottom plot, the constraint on the parameter space of Δ_6 is given by the highest invariant mass bin in $t\bar{t}$ production (shaded regions). The 68%, 95%, 99% confidence level regions are shaded in green, yellow, and orange, respectively. The best-fit contour is plotted in the green dot-dashed line. Superimposed are the 68(95)% confidence region contours of the total FBA as in Fig. 7.

at high $m_{t\bar{t}}$, this bound is to be considered as tentative at the moment. A more decisive conclusion would require a consistent evaluation of the observable at next-to-leading order in QCD including the NP contributions which is beyond the scope of this analysis.

Note that a similar constraint can also be derived from the recent CDF measurement of the $m_{t\bar{t}}$ spectrum of the FBA [47], which exhibits large positive contributions in the low top-pair invariant mass region. This poses a problem for any NP explanation of the asymmetry with heavy mediators in the $t(u)$ channels, since it will generically predict a small FBA in this region of phase space. At the moment, the significance of such a constraint is still lower than the high end tail of the production cross section spectrum, however it is potentially much more robust, since it is believed to be less sensitive to higher order QCD effects and PDF uncertainties [3].

IV. OTHER CONSTRAINTS

The constraints on color octets such as Δ_1 have been considered elsewhere in some detail [48] and we will not repeat the discussion here, noting only that they are allowed to be as light as 100 GeV. Regarding Δ_6, the most robust lower limit on its mass is given by the high energy run of LEP II, putting the lower bound at roughly $m_{\Delta_6} > 105$ GeV [49]. Tevatron searches for resonances in the invariant mass spectrum of dijets [50] only constrain the g_6^{cu} coupling. A sizable g_6^{tu} coupling does not induce flavor changing neutral current processes unless one of the other g_6^{ij} couplings is different from zero as well. Even in their presence, contributions to flavor changing neutral current processes of first-two generation up quarks such as $D - \bar{D}$ mixing only appear at one loop and we leave this for a subsequent study. Contrary to neutral t-channel mediators of $t\bar{t}$ production, the Δ_6 does not induce like-sign top-pair production which would otherwise severely constrain the high Δ_6 mass region. In addition, the single top production

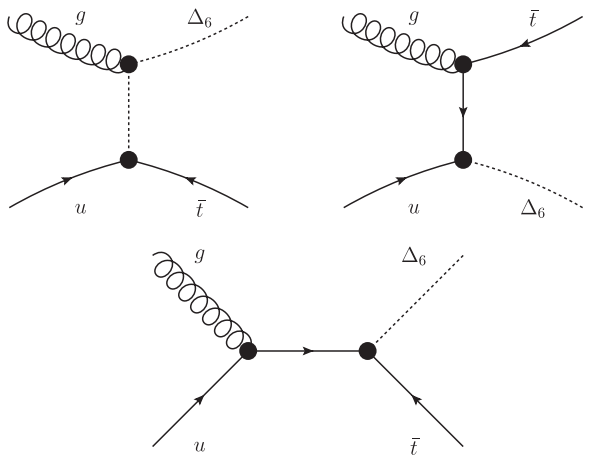

FIG. 9. Diagrams contributing to partonic single Δ_6 production, associated with an (anti)top quark.

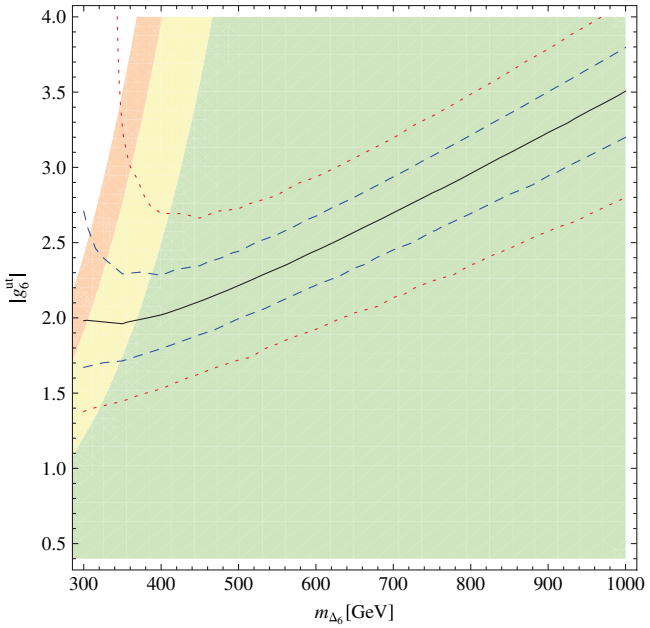

FIG. 10 (color online). Constraint on the parameter space of Δ_6 coming from $t\bar{t}$ + jet production (shaded regions). The 68%, 95%, 99% confidence level regions are shaded in green, yellow, and orange, respectively. Superimposed are the 68(95)% confidence region contours of the total $t\bar{t}$ production FBA as in Fig. 7.

cross section necessarily involves the g_6^{uc} coupling which can be suppressed. On the other hand, an important constraint on the g_6^{tu} comes from the production of $t\bar{t}$ + jet which has been measured by CDF in agreement with the SM predictions [51]. The Δ_6 contributes to this process through its associated production with a top or an antitop quark. The contributing diagrams for the latter are shown in Fig. 9. The contribution to $\sigma_{t\bar{t}+j}$ can then be written approximately as $\sigma_{t\bar{t}+j}^{\Delta_6} \approx (\sigma_{t\Delta_6^*} + \sigma_{\bar{t}\Delta_6}) \times Br(\Delta_6 \to tu)$. The expression for the underlying partonic cross section $\sigma(ug \to \bar{t}\Delta_6)$ is rather lengthy and is given in the Appendix. In case we put all other couplings of Δ_6 to zero, its branching ratio to tu pairs will be one for Δ_6 masses above the top. The above (narrow width) approximation is valid in the whole interesting parameter region provided no other channels contribute significantly to the Δ_6 width. We are also neglecting possible interference effects with the SM. This is a reasonable approximation at the Tevatron, where the dominant SM contributions come from gluon radiation and do not interfere with the Δ_6 contribution. The resulting constraint on parameters of the model is shown in Fig. 10. We see that the constraint, although not competitive at the present level of experimental precision, is potentially important for low Δ_6 masses.

V. SEARCH STRATEGIES

A detailed analysis of Δ_1 phenomenology at colliders has already been performed in Refs. [48,52], where it was

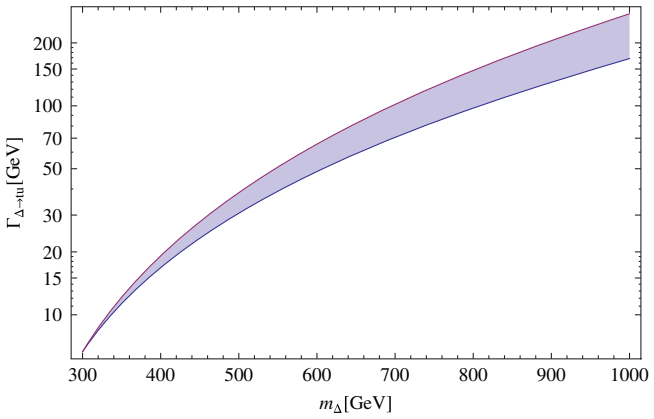

FIG. 11 (color online). Dependence of the minimal Δ_6 width on the mass of Δ_6. Values of g_6^{ut} are chosen according to Eq. (13).

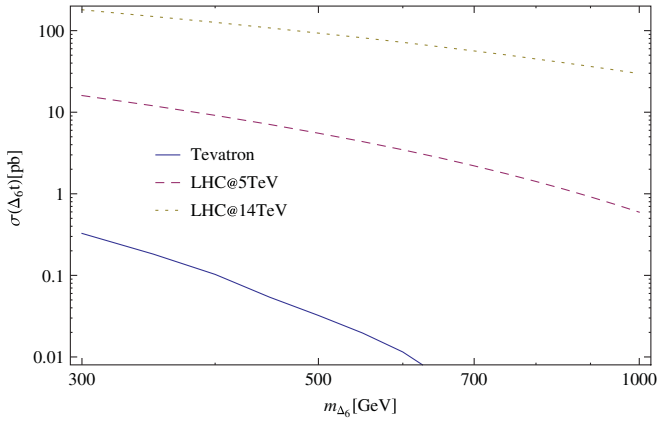

FIG. 12 (color online). Dependence of the hadronic production cross sections of $t + \Delta_6$ at the Tevatron and the LHC (for $\sqrt{s} = 5, 14$ TeV) on the mass of Δ_6. Values of g_6^{ut} are chosen according to Eq. (13).

found that such states could be observed at the LHC for masses around or below TeV. As shown in the previous sections, this is also the case in our scenario, provided that the Δ_6 is responsible for the observed deviation in the FBA.

Regarding Δ_6, in the interesting mass region its width is dominated by the two body decay $\Delta_6 \to tu$ which can be written as

$$\Gamma(\Delta_6 \to tu) = \frac{|g_6^{ut}|^2 (m_{\Delta_6}^2 - m_t^2)^2}{16\pi m_{\Delta_6}^3}. \tag{14}$$

If Δ_6 has no other relevant interactions and we neglect loop-induced decay channels, the dependence of Δ_6 width on its mass is shown in Fig. 11, where we have again taken values of g_6^{ut} which reproduce the FBA within 1 standard deviation for a given Δ_6 mass and neglected all other interactions. We see, in particular, that the Δ_6 can be narrow for low enough masses, while for masses of the order of TeV, it becomes very broad and thus more difficult to isolate in spectra.

Perhaps the most promising search strategy would be to study the spectrum of the $t\bar{t} + j$ production and search for (narrow) resonances in the invariant mass of the light jet together with a top or an antitop (m_{tj} and $m_{\bar{t}j}$). The cross sections for the production of $t + \Delta_6^*$ (or $\bar{t} + \Delta_6$) pairs at the Tevatron and the LHC are shown in Fig. 12. We see that the production cross section at the LHC is at the order of magnitude of the total SM $t\bar{t}$ cross section over the complete interesting mass range for the Δ_6 which makes this channel indeed very prospective.

The Δ_6 can also be pair produced in hadronic collisions, decaying into $t\bar{t}$ pair plus two jets. The production process proceeds though the QCD couplings of the Δ_6, so the $\Delta_6\Delta_6^*$ cross section only depends on the Δ_6 mass. At the partonic level, the $\sigma(q\bar{q} \to \Delta_6\Delta_6^*)$ and $\sigma(gg \to \Delta_6\Delta_6^*)$ read [53]

$$\sigma(q\bar{q} \to \Delta_6\Delta_6^*) = \frac{2\pi\alpha_s^2}{27\hat{s}}\hat{\beta}_\Delta^3 \tag{15}$$

$$\sigma(gg \to \Delta_6\Delta_6^*) = \frac{\pi\alpha_s^2}{96\hat{s}}\Big\{3\hat{\beta}_\Delta(3 - 5\hat{\beta}_\Delta^2) - 16\hat{\beta}_\Delta(\hat{\beta}_\Delta^2 - 2) + [8(\hat{\beta}_\Delta^4 - 1) - 9(\hat{\beta}_\Delta^2 - 1)^2] \times \log\left|\frac{\hat{\beta}_\Delta + 1}{\hat{\beta}_\Delta - 1}\right|\Big\}, \tag{16}$$

where $\hat{\beta}_\Delta = \sqrt{1 - 4m_{\Delta_6}^2/\hat{s}}$. The resulting cross sections at the Tevatron and the LHC are shown in Fig. 13. We see that the production cross section at the Tevatron only becomes sizable for very low Δ_6 masses. This channel may be more prospective at the LHC, where the cross sections of the order of 1 pb can be expected even for Δ_6 masses around 0.5 TeV. The search may be aided by the fact that the Δ_6's would appear as resonances in the invariant masses of a top quark and one of the hard jets.

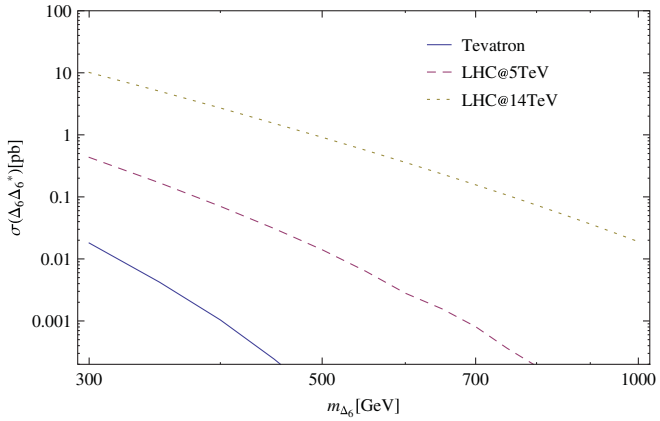

FIG. 13 (color online). Dependence of the hadronic production cross sections of $\Delta_6^*\Delta_6$ at the Tevatron and the LHC (for $\sqrt{s} = 5$, 14 TeV) on the mass of Δ_6.

VI. SUMMARY

The interplay of nonsupersymmetric $SU(5)$ GUT model which contains the 45-dimensional representation with light scalar states and the $t\bar{t}$ hadronic production phenomenology results in very interesting consequences.

Within the $SU(5)$ GUT model we found correlations between the masses of Δ_6 and Δ_1 and the partial proton decay width. In the particular scenario of a TeV scale Δ_6, present constraints also require a TeV scale Δ_1 as well. A moderate increase in the precision measurement of the $p \to e^+\pi^0$ decay width will constrain presently allowed ranges of the light scalar masses.

The contribution of Δ_6 to the production of $t\bar{t}$ at the Tevatron does not spoil the successful standard model prediction for the total hadronic cross section, whereas the associated forward-backward asymmetry can be enhanced and account for the experimental result provided the Δ_6 mass is above 300 GeV. On the other hand, some tension is already present when comparing with the high $m_{t\bar{t}}$ spectrum. The constraint gets stronger with larger Δ_6 mass, disfavoring masses above TeV. On the other hand, sizable Δ_1 contributions cannot accommodate experimental results, constraining the mass and couplings of this state. These conclusions are model independent and apply to any scenario with light scalar colored triplets and/or octets.

Some implications of the light Δ_6 scalar in the ongoing and future experiments have been discussed. The best strategy for the experimental search for this state would be to study the spectrum of the $t\bar{t}$ + jet production and search for resonances in the invariant mass of the light jet together with a top or an antitop. The Δ_6 can also be pair produced in hadronic collisions resulting in $t\bar{t}$ + 2 jets final states. This channel seems to be more promising at the LHC than at the Tevatron.

ACKNOWLEDGMENTS

I. D. would like to thank Goran Senjanović for fruitful discussions. This work is supported in part by the European Commission RTN network, Contract No. MRTN-CT-2006-035482 (FLAVIAnet), and by the Slovenian Research Agency.

Note added.—During the completion of this work, Refs. [54,55] appeared, where the effects of colored scalars on the FBA are also considered. Compared to these works, we not only study the influence of colored scalars on the FBA in a model independent way but also consider a very concrete and viable scenario, where phenomenological constraints require more than one colored scalar to be light. In addition, we study several existing and prospective future experimental constraints or signatures of Δ_6, some of which have not been considered in the aforementioned papers. In the model independent parts of our work we confirm the results of [54] and the updated version of [55].

APPENDIX: $ug \to \bar{t}\Delta_6$ AMPLITUDES

Associated production of Δ_6 in a hadron collider $ug \to \bar{t}\Delta_6$ has three contributing diagrams at tree level (Fig. 8). To avoid fermion number flowing into the $\Delta_6 \bar{u}\,\bar{t}$ vertex, one can work with the t^c field to make fermion lines going through the diagram and also correspondingly change the QCD vertex $g\bar{t}^c t^c$. For color indices arrangement $u_a g^A \to \bar{t}_b \Delta_{6c}$ the respective contributions of the three diagrams of Fig. 8 are

$$a_1 = ig_6^{ut*}\epsilon_{dbc}\left(\bar{t}^c P_R \frac{i(\not{p}_{\bar{t}} + \not{p}_{\Delta_6})}{s}[ig\gamma^\mu T^A_{da}]u\right)\epsilon^A_\mu, \tag{A1a}$$

$$a_2 = ig_6^{ut*}\epsilon_{adc}\left(\bar{t}^c[-ig\gamma^\mu T^A_{db}]\frac{i(\not{p}_u - \not{p}_{\Delta_6} + m_t)}{u - m_t^2}P_R u\right)\epsilon^A_\mu, \tag{A1b}$$

$$a_3 = ig_6^{ut*}\epsilon_{abd}(\bar{t}^c P_R u)\frac{i}{t - m^2_{\Delta_6}}[igT^A_{cd}(p_u - p_t + p_{\Delta_6})^\mu]\epsilon^A_\mu. \tag{A1c}$$

The resulting partonic differential cross section, averaged over polarizations and colors of the scattered and final state particles, is

$$\frac{d\sigma_{ug\to\bar{t}\Delta_6}}{dt} = \frac{\alpha_s|g_6^{ut}|^2}{48s^2}|\mathcal{A}_1 + \mathcal{A}_2 + \mathcal{A}_3|^2, \tag{A2}$$

where individual diagonal and interference terms are

$$|\mathcal{A}_1|^2 = \frac{m_t^2 - u}{s} \tag{A3}$$

$$|\mathcal{A}_2|^2 = \frac{(t - m_t^2)(m^2_{\Delta_6} + t)}{(t - m^2_{\Delta_6})^2} \tag{A4}$$

$$|\mathcal{A}_3|^2 = \frac{m_t^4 + 3m_t^2(m^2_{\Delta_6} - u) - m_t^2 t - su}{(u - m_t^2)^2} \tag{A5}$$

$$2\,\mathrm{Re}(\mathcal{A}_1\mathcal{A}_2^*) = -\frac{2m^2_{\Delta_6}(m_t^2 - t) - 2m_t^4 + m_t^2(s + 2t) + st}{s(m^2_{\Delta_6} - t)} \tag{A6}$$

$$2\,\mathrm{Re}(\mathcal{A}_2\mathcal{A}_3^*) = \frac{(m_t^2 - t)(m_t^2 + m^2_{\Delta_6}) - (m_t^2 + t)(m^2_{\Delta_6} - u)}{4(u - m_t^2)(t - m^2_{\Delta_6})} \tag{A7}$$

$$2\,\mathrm{Re}(\mathcal{A}_3\mathcal{A}_1^*) = 2\frac{m_t^2(s - u) - m^2_{\Delta_6}t + 2m^2_{\Delta_6}m_t^2 - us}{s(u - m_t^2)}. \tag{A8}$$

Mandelstam variables we used here are $t = (p_u - p_{\bar{t}})^2$ and $u = (p_u - p_{\Delta_6})^2$.

[1] T. Aaltonen *et al.*, CDF note 9724, 2009.

[2] T. Aaltonen *et al.* (CDF Collaboration), Phys. Rev. Lett. **101**, 202001 (2008); V. M. Abazov *et al.* (D0 Collaboration), Phys. Rev. Lett. **100**, 142002 (2008).

[3] J. H. Kuhn and G. Rodrigo, Phys. Rev. D **59**, 054017 (1999); M. T. Bowen, S. D. Ellis, and D. Rainwater, Phys. Rev. D **73**, 014008 (2006); L. G. Almeida, G. Sterman, and W. Vogelsang, Phys. Rev. D **78**, 014008 (2008).

[4] See, e.g., http://www-cdf.fnal.gov/physics/new/top/top.html, http://www-d0.fnal.gov/Run2Physics/top/.

[5] A. Djouadi, G. Moreau, F. Richard, and R. K. Singh, arXiv:0906.0604.

[6] K. Cheung, W. Y. Keung, and T. C. Yuan, Phys. Lett. B **682**, 287 (2009).

[7] S. Jung, H. Murayama, A. Pierce, and J. D. Wells, Phys. Rev. D **81**, 015004 (2010).

[8] P. H. Frampton, J. Shu, and K. Wang, Phys. Lett. B **683**, 294 (2010).

[9] I. Dorsner and I. Mocioiu, Nucl. Phys. **B796**, 123 (2008).

[10] I. Dorsner and P. F. Perez, Phys. Lett. B **642**, 248 (2006).

[11] P. Fileviez Perez, Phys. Lett. B **654**, 189 (2007).

[12] I. Dorsner, S. Fajfer, J. F. Kamenik, and N. Kosnik, Phys. Lett. B **682**, 67 (2009).

[13] H. Georgi and C. Jarlskog, Phys. Lett. B **86**, 297 (1979).

[14] E. Witten, Phys. Lett. **91B**, 81 (1980).

[15] C. T. Hill, Phys. Lett. **135B**, 47 (1984).

[16] Q. Shafi and C. Wetterich, Phys. Rev. Lett. **52**, 875 (1984).

[17] H. Georgi and S. L. Glashow, Phys. Rev. Lett. **32**, 438 (1974).

[18] S. Weinberg, Phys. Rev. D **22**, 1694 (1980).

[19] A. Giveon, L. J. Hall, and U. Sarid, Phys. Lett. B **271**, 138 (1991).

[20] I. Dorsner and P. Fileviez Perez, Phys. Lett. B **625**, 88 (2005).

[21] M. Magg and C. Wetterich, Phys. Lett. **94B**, 61 (1980).

[22] J. Schechter and J. W. F. Valle, Phys. Rev. D **22**, 2227 (1980).

[23] G. Lazarides, Q. Shafi, and C. Wetterich, Nucl. Phys. **B181**, 287 (1981).

[24] R. N. Mohapatra and G. Senjanovic, Phys. Rev. D **23**, 165 (1981).

[25] P. Minkowski, Phys. Lett. **67B**, 421 (1977).

[26] T. Yanagida, in *Proceedings of The Workshop on The Baryon Number of The Universe and Unified Theories* (Tsukuba, Japan, 1979).

[27] M. Gell-Mann, P. Ramond, and R. Slansky, in *Super-Gravity*, edited by P. van Nieuwenhuizen and D. Z. Freedman (North-Holland, Amsterdam, 1979).

[28] S. L. Glashow, NATO Advanced Study Institutes Series B: Physics **59**, 687 (1979).

[29] R. N. Mohapatra and G. Senjanovic, Phys. Rev. Lett. **44**, 912 (1980).

[30] R. Foot, H. Lew, X. G. He, and G. C. Joshi, Z. Phys. C **44**, 441 (1989).

[31] E. Ma, Phys. Rev. Lett. **81**, 1171 (1998).

[32] B. Bajc and G. Senjanovic, J. High Energy Phys. 08 (2007) 014.

[33] I. Dorsner and P. Fileviez Perez, J. High Energy Phys. 06 (2007) 029; B. Bajc, M. Nemevsek, and G. Senjanovic, Phys. Rev. D **76**, 055011 (2007).

[34] C. Amsler *et al.* (Particle Data Group), Phys. Lett. B **667**, 1 (2008).

[35] H. Nishino *et al.* (Super-Kamiokande Collaboration), Phys. Rev. Lett. **102**, 141801 (2009).

[36] A. J. Buras, J. R. Ellis, M. K. Gaillard, and D. V. Nanopoulos, Nucl. Phys. **B135**, 66 (1978).

[37] J. R. Ellis, M. K. Gaillard, and D. V. Nanopoulos, Phys. Lett. **88B**, 320 (1979).

[38] F. Wilczek and A. Zee, Phys. Rev. Lett. **43**, 1571 (1979).

[39] Y. Aoki, C. Dawson, J. Noaki, and A. Soni, Phys. Rev. D **75**, 014507 (2007).

[40] P. Fileviez Perez, H. Iminniyaz, and G. Rodrigo, Phys. Rev. D **78**, 015013 (2008).

[41] J. Kang, P. Langacker, and B. D. Nelson, Phys. Rev. D **77**, 035003 (2008).

[42] H. L. Lai *et al.* (CTEQ Collaboration), Eur. Phys. J. C **12**, 375 (2000).

[43] T. Aaltonen *et al.*, CDF note 9448, 2009.

[44] M. Cacciari, S. Frixione, M. L. Mangano, P. Nason, and G. Ridolfi, J. High Energy Phys. 09 (2008) 127; N. Kidonakis and R. Vogt, Phys. Rev. D **78**, 074005 (2008); S. Moch and P. Uwer, Nucl. Phys. B, Proc. Suppl. **183**, 75 (2008).

[45] R. Frederix and F. Maltoni, J. High Energy Phys. 01 (2009) 047.

[46] T. Aaltonen *et al.* (CDF Collaboration), Phys. Rev. Lett. **102**, 222003 (2009).

[47] T. Aaltonen *et al.*, CDF note 9853, 2009.

[48] A. V. Manohar and M. B. Wise, Phys. Rev. D **74**, 035009 (2006); C. P. Burgess, M. Trott, and S. Zuberi, J. High Energy Phys. 09 (2009) 082.

[49] J. M. Arnold, M. Pospelov, M. Trott, and M. B. Wise, arXiv:0911.2225.

[50] T. Aaltonen *et al.* (CDF Collaboration), Phys. Rev. D **79**, 112002 (2009).

[51] T. Aaltonen *et al.*, CDF note 9850, 2009.

[52] M. I. Gresham and M. B. Wise, Phys. Rev. D **76**, 075003 (2007); M. Gerbush, T. J. Khoo, D. J. Phalen, A. Pierce, and D. Tucker-Smith, Phys. Rev. D **77**, 095003 (2008); P. Fileviez Perez, R. Gavin, T. McElmurry, and F. Petriello, Phys. Rev. D **78**, 115017 (2008); A. Idilbi, C. Kim, and T. Mehen, Phys. Rev. D **79**, 114016 (2009).

[53] C. R. Chen, W. Klemm, V. Rentala, and K. Wang, Phys. Rev. D **79**, 054002 (2009).

[54] J. Shu, T. M. P. Tait, and K. Wang, Phys. Rev. D **81**, 034012 (2010).

[55] A. Arhrib, R. Benbrik, and C. H. Chen, arXiv:0911.4875.